

MOLECULAR GAS DISTRIBUTION IN A PROTOGALAXY CANDIDATE IRAS F10214+4724: A DENSE COMPACT NUCLEUS AND NONDETECTED EXTRA COMPONENTS

KAZUSHI SAKAMOTO,^{1,2} SUMIO ISHIZUKI,^{1,2} RYOHEI KAWABE,² AND MASATO ISHIGURO²

Received 1992 June 1; accepted 1992 July 9

ABSTRACT

Following the paper by Kawabe et al. the results of aperture synthesis observations of CO($J = 3 \rightarrow 2$) emission in IRAS F10214+4724, with the Nobeyama Millimeter Array (NMA), are reported. CO($J = 3 \rightarrow 2$) emission is detected only at the blueshifted half of the CO($J = 3 \rightarrow 2$) velocity range reported in previous single-dish observations; the redshifted half is not detected in our observations. The detected CO($J = 3 \rightarrow 2$) emission is located at a VLA and optical position and shows a compact shape. This component contains $(3\text{--}15) \times 10^{11} h^{-2} M_{\odot}$ of molecular gas and has a beam deconvolved size $12 h^{-1}$ kpc in diameter. The molecular gas surface density is as high as that in infrared luminous galaxies. The nondetected component must have brightness temperatures lower than the sensitivity and is probably extended or composed of a number of subcomponents. The molecular gas distribution suggests that IRAS F10214+4724 is an interacting or merging system.

Subject headings: galaxies: formation — galaxies: individual (IRAS F10214+4724) — galaxies: interstellar matter — infrared: galaxies

1. INTRODUCTION

A high-redshift, huge luminosity IRAS galaxy F10214+4724 discovered by Rowan-Robinson et al. (1991) is at $z = 2.286$ and has a total infrared luminosity $L_{\text{FIR}} = 7.5 \times 10^{13} h^{-2} L_{\odot}$ (cosmological parameters $H_0 = 100 h \text{ km s}^{-1} \text{ Mpc}^{-1}$ and $q_0 = 0.5$ are assumed through this *Letter*). The following detection of CO($J = 3 \rightarrow 2$) emission from IRAS F10214+4724 at the NRAO 12 m telescope (Brown & Vanden Bout 1991) revealed that it was extremely gas rich and made it an ideal target for millimeter-wave interferometers to study the genesis and evolution of galaxies. Inspired by the detection, we tried aperture synthesis observations of the CO($J = 3 \rightarrow 2$) line to determine distribution and kinematics of molecular gas in IRAS F10214+4724.

Details of observations and preliminary results were reported by Kawabe et al. (1992, hereafter Paper I). In Paper I, it is reported that a compact CO($J = 3 \rightarrow 2$) emission was detected at a redshift around $z = 2.286$ at the VLA source position and the detected line flux was less than half of the flux measured at the NRAO 12 m telescope. In this *Letter*, we examine velocity channel maps and spectrum. We then discuss distribution of molecular gas and the reason that more than half the flux was missed. We also discuss the origin of the powerful infrared emission in the light of the molecular content.

2. OBSERVATIONS AND RESULTS

Aperture synthesis observations were made during 1992 January 21–25 and February 19–24 using the Nobeyama Millimeter Array (NMA). We observed CO($J = 3 \rightarrow 2$) emission (rest frequency 345.7960 GHz) redshifted to around 105.2 GHz ($z = 2.286$). The resolution and the primary beam are $8''.9 \times 6''.0$ and about $70''$ in half-power beamwidth, respectively. Details of the observations are described in Paper I.

¹ Department of Astronomy, University of Tokyo, Bunkyo-Ku, Tokyo 113, Japan.

² Nobeyama Radio Observatory, Minamimaki, Minamisaku, Nagano 384-13, Japan. Nobeyama Radio Observatory (NRO) is a branch of the National Astronomical Observatory, the Ministry of Education, Science, and Culture of Japan.

Velocity channel maps of CO($J = 3 \rightarrow 2$) emission from IRAS F10214+4724 are shown in Figure 1. The integration velocity width of each map is 185 km s^{-1} and velocity increments between adjacent maps are half of the integration width, 92.5 km s^{-1} ; a velocity is doubly sampled for improvement of signal-to-noise ratio. The maps cover from -301 to $+531 \text{ km s}^{-1}$ (the zero velocity corresponds to 105.2331 GHz, $z = 2.2860$) including the whole velocity range where CO($J = 3 \rightarrow 2$) emission was detected with a 12 m single-dish telescope by Brown & Vanden Bout (1991), from -115 to $+250 \text{ km s}^{-1}$. The maps show there is a compact CO emission associated with the positions of an optical object ("object F") and a VLA source in Rowan-Robinson et al. (1991) and the emission appears only in three maps with central velocities -116 , -24 , and $+69 \text{ km s}^{-1}$. We will refer to this emission as the "nuclear compact component." The positions of centroids of the CO emission in the three adjacent maps appear to shift from each other, but this is not significant taking account into the possible fluctuation of the visibility phase due to the low signal-to-noise ratio; in other words, we do not detect a significant velocity gradient of the molecular gas. Though the CO spectrum of Brown & Vanden Bout (1991) shows the CO emission at the redshifted half ($v = +68$ to $+250 \text{ km s}^{-1}$) of the profile has a comparable CO flux to the blueshifted half ($v = -115$ to $+68 \text{ km s}^{-1}$), the CO emission at the redshifted half cannot be seen anywhere in our channel maps.

In Figure 2, measured brightness temperatures of peaks in channel maps are shown and compared with the single-dish spectrum obtained by Brown & Vanden Bout (1991). Since the mapped CO emission is not resolved, the peak brightness temperatures give a spectrum of the whole CO of the nuclear compact component. The spectrum illustrates that the emission from the nuclear compact component corresponds to the blueshifted half of the single-dish CO line profile. We estimated the CO line width of the nuclear compact component to be about 200 km s^{-1} and the central velocity of the CO emission to be $-25 \pm 20 \text{ km s}^{-1}$. This central velocity corresponds to a redshift $z = 2.2858 \pm 0.0002$.

Since the CO detected velocity width is narrow, about 200

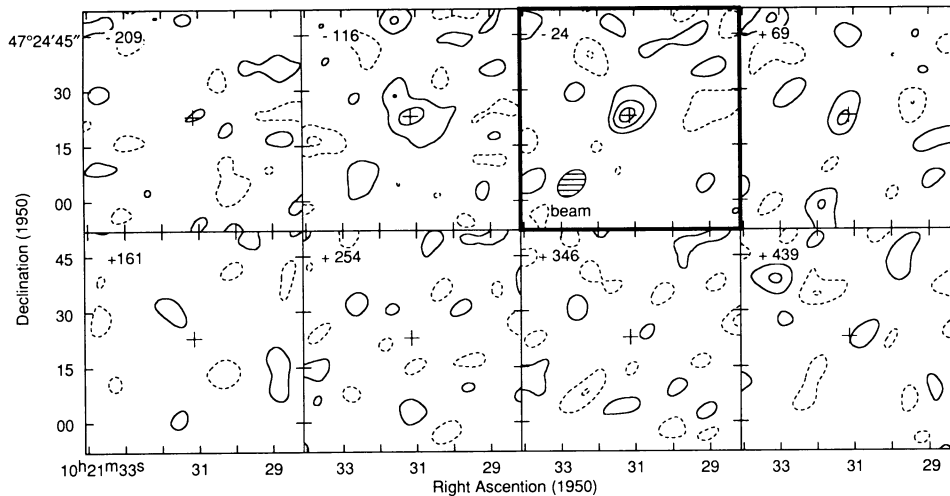


FIG. 1.—Channel CO intensity maps of IRAS F10214+4724 integrated over a velocity width of 185 km s^{-1} . Central velocities of each map are denoted in each frame and the velocities refers to 105.2331 GHz ($z = 2.2860$). Contour levels are $\pm 1.5 \sigma$, $\pm 3 \sigma$, and 4.5σ ($1 \sigma = 15 \text{ mK}$). The cross marks the phase tracking center (the VLA position: Rowan-Robinson et al. 1991). A hatched ellipse represents the synthesized beam, $8''.9 \times 6''.0$ (HPBW) with a PA 132° . The channel map for $v = -24 \text{ km s}^{-1}$, in a thick frame, is an integrated intensity map.

km s^{-1} , the channel map with a central velocity -24 km s^{-1} is an integrated CO intensity map. In the map, the peak intensity of the nuclear compact component is about 5 times the rms noise. The position of the nuclear compact component is R.A. = $10^{\text{h}}21^{\text{m}}31^{\text{s}}.2$, decl. = $+47^\circ24'23''$ ($\pm 1''$). It coincides with the positions of the VLA source and the optical object (“object F”) (Rowan-Robinson et al. 1991) within $1''.2$. The integrated line flux is $(10 \pm 2.5) \text{ Jy km s}^{-1}$. This $\text{CO}(J = 3 \rightarrow 2)$ flux is about 40% of the single-dish total CO flux³ and about 80% of the single-dish flux of the blueshifted half. The flux of the nuclear compact component corresponds to a $\text{CO}(J = 3 \rightarrow 2)$ luminosity of $8.4 \times 10^7 h^{-2} L_\odot$.

We measured dimensions and orientations of the nuclear compact component in the integrated intensity map and analytically deconvolved them with our synthesized beam. The beam deconvolved size of the nuclear compact component is $3'' \pm 0''.5$ ($= [12 \pm 2] h^{-1} \text{ kpc}$) in diameter at half-maximum. It is comparable to the size of the optical image, $4''$ (Rowan-Robinson et al. 1991). The deconvolved size is, however, an upper limit of the intrinsic size because of the possible scatters of visibility phases during observations due to receiver noise and atmospheric fluctuation.

3. DISCUSSION

3.1. Nature of the Nuclear Compact Component

We made an estimate of molecular gas mass $M(\text{H}_2)$ using a Galactic $\text{CO}(J = 1 \rightarrow 0)$ to H_2 conversion factor $\alpha = 4.5 M_\odot (\text{K km s}^{-1} \text{ pc}^2)^{-1}$. Substituting the observed $\text{CO}(J = 3 \rightarrow 2)$ flux into a formula in Solomon, Radford, & Downes (1992) derived on the assumption that brightness temperatures of $\text{CO}(J = 3 \rightarrow 2)$ and $\text{CO}(J = 1 \rightarrow 0)$ are the same, the molecular gas mass in the nuclear compact component is calculated to be $M(\text{H}_2) = 3 \times 10^{11} h^{-2} M_\odot$. However, it is not evident that the two lines have the same brightness temperature. Since the critical density and the upper state energy level of

$\text{CO}(J = 3 \rightarrow 2)$ are different from those of $\text{CO}(J = 1 \rightarrow 0)$, it is possible that $\text{CO}(J = 3 \rightarrow 2)$ traces only a high-temperature and high-density portion of molecular gas. We then tried another estimate of molecular gas mass in addition on a simple assumption that $\text{CO}(J = 3 \rightarrow 2)$ luminosity to molecular gas mass ratio has an equal value both in our Galaxy and in IRAS F10214+4724. A $\text{CO}(J = 3 \rightarrow 2)$ luminosity of our Galaxy derived by COBE observations is $10^{5.1} L_\odot$ (Wright et al. 1991), and the total mass of molecular gas in our Galaxy is $2.3 \times 10^9 M_\odot$ (Scoville & Sanders 1987). Therefore another estimate of the molecular gas mass of the nuclear compact component is $1.5 \times 10^{12} h^{-2} M_\odot$.

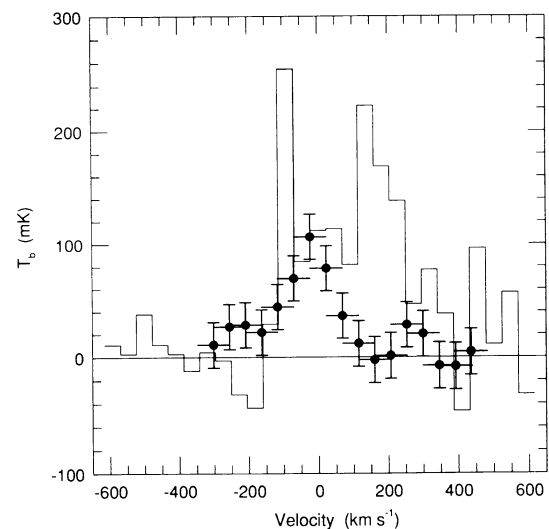


FIG. 2.—Spectrum of $\text{CO}(J = 3 \rightarrow 2)$ emission observed at the Nobeyama Millimeter Array, plotted over the single-dish spectrum (Brown & Vanden Bout 1991) obtained at the NRAO 12 m telescope. The brightness temperatures are measured at the position of nuclear compact component. The velocity scale refers to 105.2331 GHz . Horizontal bars show the velocity ranges of averaging, 92.5 km s^{-1} , and vertical bars represent rms noise, 20 mK . The single-dish spectrum is scaled to the NMA scale through the NRAO’s T_R^* scale on the assumption that the source is a pointlike source.

³ In Brown & Vanden Bout (1991), the total CO flux measured at the NRAO 12 m telescope was written as 21 Jy km s^{-1} . But the correct value is $26 \text{ Jy km s}^{-1} = 35 \text{ Jy K}^{-1} \times 0.74 \text{ K km s}^{-1}$ (P. A. Vanden Bout, private communication).

As pointed out by many authors (e.g., Maloney 1990), there is no empirical basis for the use of “standard” conversion factor, α , to an infrared luminous galaxy in early cosmological epoch where metallicity, temperature, and density of molecular gas must differ from those of giant molecular clouds in our Galaxy. The estimate from CO($J = 3 \rightarrow 2$) luminosity is not on an empirical basis, either. Therefore the estimate of the molecular gas mass may well have an error of an order of magnitude besides the error coming from the ambiguity of cosmological parameters. With this in mind, we use the molecular gas mass derived above, $(3-15) \times 10^{11} h^{-2} M_{\odot}$, as a moderate estimate.

A dynamical mass of the nuclear compact component is estimated to be $M_{\text{dyn}} = 1.4 \times 10^{10} h^{-1} \sin^{-2} i M_{\odot}$ from the size and the line width, where i is the inclination of the disk. The ratio of gas to dynamical masses of the nuclear compact component is

$$\frac{M(\text{H}_2)}{M_{\text{dyn}}} = (11 - 54) \left[\frac{1}{h} \right] \left[\frac{0.5}{\sin^2 i} \right] \left[\frac{3''}{\theta} \right],$$

where θ is the angular diameter of the nuclear compact component. Since this ratio must be less than unity, we infer that the galaxy is almost face-on unless the molecular gas mass is not overestimated.

Surface density of molecular gas is calculated to be $\Sigma(\text{H}_2) = (3-13) \times 10^3 M_{\odot} \text{pc}^{-2}$ assuming the diameter equals to the beam deconvolved CO size, $3'' = 12 h^{-1} \text{kpc}$. This gas surface density of the nuclear compact component is as high as that of infrared luminous galaxies, which are mostly mergers or interacting galaxies and have AGN activities and/or starburst characteristics.

Only with molecular gas, the mass of the nuclear compact component exceeds or equals the total (star + gas) mass of our Galaxy. On the other hand, its extent is of the same order of the size of our Galaxy. Since the optical image (Rowan-Robinson et al. 1991) indicates the existence of stars, the nuclear compact component must have a larger total mass than our Galaxy and will evolve into a massive galaxy with high stellar density.

3.2. Where Is the Missing Redshifted Component?

We detected a compact component with a line width about 200 km s^{-1} which corresponds to the blueshifted half of the single-dish spectrum previously obtained by Brown & Vanden Bout (1991) at the NRAO 12 m telescope, but did not detect a component which is in charge of the redshifted half of the single-dish spectrum. Where is the missing redshifted component? Since the primary beam of the NMA is larger than that of the NRAO 12 m telescope, the component which emits the missing redshifted half must be in our field of view. If the missing component were a single component much smaller than our synthesized beam and had brightness temperatures expected from the blueshifted half of the single-dish spectrum, it should have been detected as a 10σ peak in a channel map. Therefore the missing redshifted flux does not come from a single compact object. As a consequence, there remain three possibilities for the origin of the redshifted flux: (1) the CO emission is so extended that it is resolved out; (2) though it is not resolved out, it is extended and the CO brightness temperature is too low to be detected; and (3) there are several subcomponents other than the nuclear compact component and each one has lower CO brightness temperatures than our sensitivity. In either case, the observations suggest that molec-

ular gas of IRAS F10214+4724 consists of at least two components, the detected nuclear compact component and the missed extra component(s). Since their projected separation is less than $30'' (= 120 h^{-1} \text{kpc})$, half of the NRAO beam, and their separation in velocity is only 200 km s^{-1} , their association must not be a coincidence.

We can constrain the distribution of extra component(s) from a comparison between the single-dish and interferometer spectra, that is, the extra component(s) must distribute asymmetrically with respect to the nuclear compact component. It is because that the velocities of the missing component are not symmetrical with respect to the velocity of the nuclear compact component. For example, a symmetrical body of molecular gas rotating around or infalling to the nuclear compact component is impossible. Also, a large number of extra components which have random motions around the nuclear compact component like galaxies around a cD galaxy can be ruled out.

Multiple-component distribution of molecular gas is familiar in infrared luminous galaxies and thought to be evidence for merging or interaction. For example, Arp 55 (Sanders et al. 1988a) and VV 114 (Scoville et al. 1989) have two peaks of CO emission separated by 4–13 kpc, in particular, one of the two CO peaks of VV 114 does not have a significant optical counterpart, which may be the case in IRAS F10214+4724; and Arp 299 (Sargent & Scoville 1991) has two nuclei and three subcomponents within about 7 kpc. Similar to such infrared luminous galaxies, IRAS F10214+4724 is possibly a large-scale interacting or merging system and its source of the huge infrared luminosity may be fueled by the molecular gas which has concentrated to the nuclear region to form the dense compact component as a result of merging or interaction.

On the assumption that the nuclear compact component and the extra components are gravitationally bound, an estimate of their separation can be calculated:

$$r = 27'' \left[\frac{h}{1} \right] \left[\frac{v}{200 \text{ km s}^{-1}} \right]^{-2} \left[\frac{M}{10^{12} M_{\odot}} \right],$$

where v is a circular velocity and M is the total mass associated with the nuclear compact component. If the orbit of the extra components has some inclination, the circular velocity will be larger than 200 km s^{-1} and the separation will be reduced.

3.3. Origin of the Huge Infrared Luminosity

Figure 3 is an $L_{\text{IR,tot}}/M_{\text{nuc}}(\text{H}_2)$ -to- $\Sigma_{\text{nuc}}(\text{H}_2)$ relation diagram of infrared luminous galaxies. It shows that the high molecular gas surface density of IRAS F10214+4724 is comparable to infrared-luminous galaxies. This supports an idea that the gas is concentrated highly enough to produce high infrared luminosity as in infrared-luminous galaxies. Since most infrared-luminous galaxies are interacting or merging, it is possible that the huge luminosity of IRAS F10214+4724 is also triggered by a galaxy interaction or merging process. Galaxy interactions and mergings are thought to transport gas toward galaxy centers to trigger starburst or fuel active galactic nuclei (e.g., Sanders et al. 1988b). An unknown object with the missing redshifted flux is likely a perturber which causes a high concentration of molecular gas and high energy output of IRAS F10214+4724.

Since the discovery of a huge infrared luminosity, $\sim 10^{14} L_{\odot}$, of IRAS F10214+4724, it has remained to answer what the energy source is. The molecular gas and infrared properties prefer that the huge infrared luminosity is due to an active galactic nucleus as discussed below.

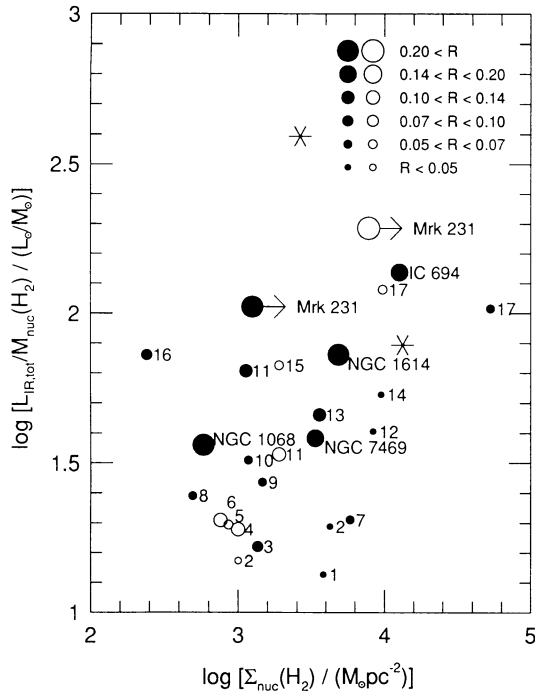


FIG. 3.—An $L_{\text{IR,tot}}/M_{\text{nuc}}(\text{H}_2)$ to $\Sigma_{\text{nuc}}(\text{H}_2)$ relation diagram for infrared-luminous galaxies, where $L_{\text{IR,tot}}$ is a total luminosity obtained from *IRAS* observations, M_{H_2} is a mass of molecular gas in a nuclear region derived from interferometric observations, and $\Sigma_{\text{nuc}}(\text{H}_2)$ is a molecular gas surface density in the same nuclear region. The two asterisks represent IRAS F10214+4724. $L_{\text{IR,tot}} = 1.2 \times 10^{14} h^{-2} L_{\odot}$ in case B by Rowan-Robinson et al. (1991) and Clements et al. (1992) is used. The upper left and lower right asterisks correspond to the $M_{\text{nuc}}(\text{H}_2)$ estimates of $3 \times 10^{11} M_{\odot}$ and $15 \times 10^{11} M_{\odot}$, respectively. The closed and open circles represent the samples quoted from Scoville et al. (1991) and Okumura et al. (1991) respectively. The circles with figures represent (1) NGC 3079, (2) NGC 828, (3) NGC 2146, (4) Mrk 331, (5) NGC 695, (6) NGC 6090, (7) NGC 520, (8) Arp 55, (9) NGC 4038/39, (10) VII Zw 31, (11) NGC 6240, (12) Zw 049.057, (13) VV 144, (14) IRAS 17208–0014, (15) NGC 2623, (16) IRAS 10173+0828, and (17) Arp 220. A CO($J = 1 \rightarrow 0$) to H_2 conversion factor $\alpha = 4.5 M_{\odot} (\text{K km s}^{-1} \text{pc}^2)^{-1}$ is used for all the quoted samples. The size of the circles represents the 25 to 100 μm flux ratio as shown upper right in the frame.

In Figure 3, if we take sample galaxies with the same molecular gas surface densities, there is a trend that the galaxies with high $L_{\text{IR,tot}}/M_{\text{nuc}}(\text{H}_2)$ ratios have high 25 to 100 μm flux ratios

(the size of the circles represents the 25 to 100 μm flux ratio). In other words, in a galaxy with a higher efficiency of energy production than expected from its molecular gas surface density, 25 μm flux is relatively strong. This correlation suggests that such a galaxy has an efficient energy source for mid-infrared luminosity. We call such a galaxy a *high-efficiency mid-infrared galaxy*. Mrk 231, NGC 1068, NGC 1614, NGC 7469, and IC 694, which are all with $F_{\nu}(25 \mu\text{m})/F_{\nu}(100 \mu\text{m}) > 0.15$ are examples of high-efficiency mid-infrared galaxies in Figure 3. IRAS F10214+4724 has a mid-infrared excess in its infrared spectrum with $F_{\nu}(25 \mu\text{m})/F_{\nu}(100 \mu\text{m}) = 0.30 \pm 0.10$ (Clements et al. 1992). In addition, IRAS F10214+472 has an $L_{\text{IR,tot}}/M_{\text{nuc}}(\text{H}_2)$ ratio larger or no less than the high-efficiency mid-infrared galaxies. Thus IRAS F10214+4724 is suggested to belong to a family of high-efficiency mid-infrared galaxies.

Galaxies with mid-infrared excesses are associated with active galactic nuclei. For example, the high-efficiency mid-infrared galaxies appeared in Figure 3 are associated with active galactic nuclei; Mrk 231 is a quasar; NGC 1068, NGC 1614, and NGC 7469 are Seyfert galaxies; and IC 694 is suggested to have an active nucleus (Sargent et al. 1987). In addition, warm samples in Sanders et al. (1988c), with $F_{\nu}(25 \mu\text{m})/F_{\nu}(100 \mu\text{m}) = 0.20\text{--}0.86$, are all Seyfert galaxies [they are in striking contrast to the six galaxies with $F_{\nu}(25 \mu\text{m})/F_{\nu}(100 \mu\text{m}) = 0.05\text{--}0.12$, including Arp 220 with $F_{\nu}(25 \mu\text{m})/F_{\nu}(100 \mu\text{m}) = 0.07$, in Sanders et al. (1988b)]. Such an association of mid-infrared excesses with active galactic nuclei is clearly illustrated by Hutchings & Neff (1991).

Therefore, high-efficiency mid-infrared galaxies should be associated with active galactic nuclei. Their high $L_{\text{IR,tot}}/M_{\text{nuc}}(\text{H}_2)$ ratios or high efficiencies should come from their active galactic nuclei. From this point of view, it is plausible that the huge infrared luminosity of IRAS F10214+4724 is due to an active galactic nucleus, probably a quasar. Gas consumption time scale due to an active galactic nuclei can be another support for the argument; the time scale is long enough to support the huge infrared luminosity as discussed in Paper I.

We express our thanks to all the members who engaged in the development and operation of the Nobeyama Millimeter Array. S. I. is supported by the Japan Society for the Promotion of Science.

REFERENCES

- Brown, R. L., & Vanden Bout, P. A. 1991, *AJ*, 102, 1956
 Clements, D. L., Rowan-Robinson, M., Lawrence, A., Broadhurst, T., & McMahon, R. 1992, *MNRAS*, 256, 35
 Hutchings, J. B., & Neff, S. G. 1991, *AJ*, 101, 434
 Kawabe, R., Sakamoto, K., Ishizuki, S., & Ishiguro, M. 1992, *ApJ*, 397, L23 (Paper I)
 Maloney, P. 1990, in *The Interstellar Medium in Galaxies*, ed. H. A. Thronson & J. M. Shull (Dordrecht: Kluwer), 493
 Okumura, S. K., Kawabe, R., Ishiguro, M., Kasuga, T., Morita, K.-I., & Ishizuki, S. 1991, in *Dynamics of Galaxies and Their Molecular Cloud Distributions*, ed. F. Combes & F. Casoli (Dordrecht: Kluwer), 425
 Rowan-Robinson, M., et al. 1991, *Nature*, 351, 719
 Sanders, D. B., Scoville, N. Z., Sargent, A. I., & Soifer, B. T. 1988a, *ApJ*, 324, L55
 Sanders, D. B., Soifer, B. T., Elias, J. H., Madore, B. F., Matthews, K., Neugebauer, G., & Scoville, N. Z. 1988b, *ApJ*, 325, 74
 Sanders, D. B., Soifer, B. T., Elias, J. H., Neugebauer, G., & Matthews, K. 1988c, *ApJ*, 328, L35
 Sargent, A. I., Sanders, D. B., Scoville, N. Z., & Soifer, B. T. 1987, *ApJ*, 312, L35
 Sargent, A. I., & Scoville, N. Z. 1991, *ApJ*, 366, L1
 Scoville, N. Z., & Sanders, D. B. 1987, in *The Interstellar Processes*, ed. D. J. Hollenbach & H. A. Thronson, Jr. (Dordrecht: Reidel), 21
 Scoville, N. Z., Sanders, D. B., Sargent, A. I., Soifer, B. T., & Tinney, C. G. 1989, *ApJ*, 345, L25
 Scoville, N. Z., Sargent, A. I., Sanders, D. B., & Soifer, B. T. 1991, *ApJ*, 366, L5
 Solomon, P. M., Radford, P. M., & Downes, D. 1992, *Nature*, 356, 318
 Wright, E. L., et al. 1991, *ApJ*, 381, 200

Note added in proof.—The flux density of the calibrator 0923+392 was checked again and found to be 4.5 ± 0.7 Jy. Since 6.0 Jy is assumed throughout Papers I and II, the flux and other values derived from the flux should be changed by a factor of 0.75, though this does not affect the discussion.